Recrystallization of ice enhances the creep and vulnerability to fracture of ice shelves

Meghana Ranganathan[a], Brent Minchew[a], Colin R. Meyer[b], Matěj Peč[a]

[a] *Department of Earth, Atmospheric and Planetary Sciences, Massachusetts Institute of Technology, 77 Massachusetts Ave, Cambridge, 02139, MA, USA*
[b] *Thayer School of Engineering, Dartmouth College, 14 Engineering Dr, Hanover, 03755, NH, USA*

Abstract

The initiation of fractures and fast flow in floating regions of Antarctica have the potential to destabilize large regions of the grounded ice sheet, leading to rapid sea-level rise. While observations have shown rapid, localized deformation and damage in the margins of fast-flowing glaciers, there remain gaps in our understanding of how rapid deformation affects the viscosity and toughness of ice. Here we derive a model for dynamic recrystallization of ice that includes a novel representation of migration recrystallization. This mechanism is absent from existing models and is likely dominant in warm areas undergoing rapid deformation, such as shear margins in ice sheets. While solid earth studies find fine-grained rock in shear zones, here we find elevated ice grain sizes (> 10 mm) due to warmer temperatures and high strain rates activating migration recrystallization. Large grain sizes imply that ice in shear margins deforms primarily by dislocation creep, suggesting a flow-law stress exponent of $n \approx 4$ rather than the canonical $n = 3$. Further, we find that this increase in grain size results in a decrease in tensile strength of ice by $\sim 75\%$ in the margins of glaciers. Thus, this increase in grain size softens the margins of fast-flowing glaciers and makes ice shelf margins more vulnerable to fracture than previously supposed. These results also suggest the need to consider the effects of dynamic recrystallization in large-scale ice-sheet modeling.

Keywords: glaciers, fracture, recrystallization, creep

PACS: 0000, 1111

2000 MSC: 0000, 1111

---

1. Introduction

Ice shelves, the floating regions of large ice sheets, provide a significant control on the evolution of ice sheets and their contributions to sea-level rise. Ice shelves restrain (i.e., buttress) the upstream grounded portions of the ice sheet, preventing rapid flow of grounded ice towards the ocean. Calving events and dynamic thinning reduce the buttressing that ice shelves provide to the grounded ice, resulting in accelerated flow and possible instability of the ice sheet. Thus, a combination of ice fracture and accelerated flow may play a significant role in controlling the stability of the West Antarctic Ice Sheet (Thomas and Bentley, 1978; Wingham et al., 2009; Pollard et al., 2015; Gudmundsson et al., 2019).

Fracture and flow generally occur in areas of rapid deformation, which appears in the margins of fast-flowing glaciers and ice shelves (known as *shear margins*). A significant concentration of fractures and damage on ice shelves are found in the margins, which may have implications for the stability of the ice shelf (Lhermitte et al., 2020). Further, the lateral shearing that occurs in shear margins of grounded glaciers provides a control on flow speed and contributes to the buttressing effect (MacAyeal, 1989; Ranganathan et al., 2021). While this has been well-observed, there remains uncertainty in the physical processes underlying fracturing and accelerated flow in shear margins.

Fundamentally, the creep and fracture of ice are dictated by the grain-scale microstructure of the ice. It is well-known from solid earth studies that the physical properties of the crystalline microstructure - including grain size and grain orientation - affect the rates of creep and fracture of rocks significantly (Van der Wal et al., 1993; De Bresser et al., 2001; Montési and Hirth, 2003) and modeling and laboratory studies have proposed similar effects in ice (e.g. (Currier and Schulson, 1982; Cuffey et al., 2000; Goldsby and Kohlstedt, 2001; Hruby et al., 2020; Behn et al., 2020)). However, the physics of the microstructure of ice has rarely been applied to the question of how rapid deformation induces positive feedbacks on flow and how areas of rapid deformation fracture. Here, we study the effect that deformation-induced grain size evolution may have on flow and fracture of ice.

Observations show that grains are large in areas of glaciers where ice is warm and being sheared. Measurements of grain size in the GRIP (Greenland Ice Core Project) ice core and GISP2 (Greenland Ice Sheet Project 2) ice core shows that grain sizes increase rapidly with depth near the base, where the ice is frozen to the bed and thus strain rates are relatively large and the ice is warm (Thorsteinsson et al., 1997; Gow et al., 1997). We would therefore expect grains to be large in shear margins, where strain rates are quite high (Gardner et al., 2018) and consequently the ice is warmed, sometimes to the melting point, through viscous dissipation (Meyer and Minchew, 2018). While there are no observations of grain size at depth in shear margins, measurements made in shallow boreholes (Jackson and Kamb, 1997) and observations of grain size in temperate glaciers (Tison and Hubbard, 2000) support the suggestion that grains are likely large in shear margins.

Grain size influences the mechanisms of creep that allow ice to flow as a viscous fluid (Goldsby and Kohlstedt, 2001). Most known creep mechanisms, such as diffusion creep and grain-boundary sliding, have explicit and well-tested grain size dependencies. On the other hand, numerous laboratory experiments have shown that dislocation creep is practically independent of grain size (Duval and Gac, 1980; Jacka, 1984). For grain-size-dependent mechanisms, creep deformation is enhanced as grain sizes get smaller and diminished as grain sizes grow. Therefore, the relative influence of dislocation creep increases as grains grow and we may expect that areas of large grain sizes will deform primarily by dislocation creep, a consideration with important implications for the viscosity of ice. Since rates of shearing in shear margins affect the flow speed of grounded ice and may affect the buttressing of ice shelves, grain size in shear margins may also affect ice shelf evolution.

Furthermore, the tendency for ice to fracture is a function of the size and distribution of flaws, where stresses intensify. Larger flaw sizes tend to increase the stress intensity, implying that in general, the tensile strength of ice decreases as the flaw size increases. For intact or pristine ice, the flaw size is set by the grain size, and therefore the tensile strength of ice decreases as grain size increases, consistent with laboratory studies (Figure 3a) (Currier and Schulson, 1982; Nixon and Schulson, 1987, 1988). Thus, we might suppose that glacier shear margins are likely to have relatively large grain sizes that will decrease the tensile strength of the ice and could explain the observations of crevassing and fracture (e.g. Lhermitte et al. (2020)). Here, we derive a model for steady-state grain size in deforming glacier ice to consider the effect that grain size may have on the creep and vulnerability of ice to fracture in shear margins of rapidly-deforming glaciers.

2. A Steady-State Grain Size Model

Recrystallization processes alter the orientation and size of ice grains both in the absence of and in response to deformation. While there are many mechanisms of recrystallization, three main processes likely dominate the evolution of grain size in ice: normal grain growth, grain-size reduction, and migration recrystallization (Duval and Castelnau, 1995). Thus the net rate of change in grain size can be described as the sum of the contributions from all mechanisms, assuming that these mechanisms operate independently, as past work has assumed (Austin and Evans, 2007):

$$\dot{d} = \dot{d}_{\mathrm{red}} + \dot{d}_{\mathrm{mig}} + \dot{d}_{\mathrm{nor}} \tag{1}$$

where overdots represent time derivatives, $\dot{d}_{\mathrm{nor}}$ is the rate of change in grain size due to normal grain growth, $\dot{d}_{\mathrm{red}}$ is the rate of change in grain size due to grain-size reduction, and $\dot{d}_{\mathrm{mig}}$ is the rate of change in grain size due to migration recrystallization. We note that there are multiple proposed mechanisms for grain size reduction (subgrain rotation by rotation recrystallization is well-known in studies of ice (Derby and Ashby, 1987; Duval and Castelnau, 1995; De La Chapelle et al., 1998; De Bresser et al., 1998; Montagnat and Duval, 2000), and other mechanisms include nucleation of grains by bulging) (De La

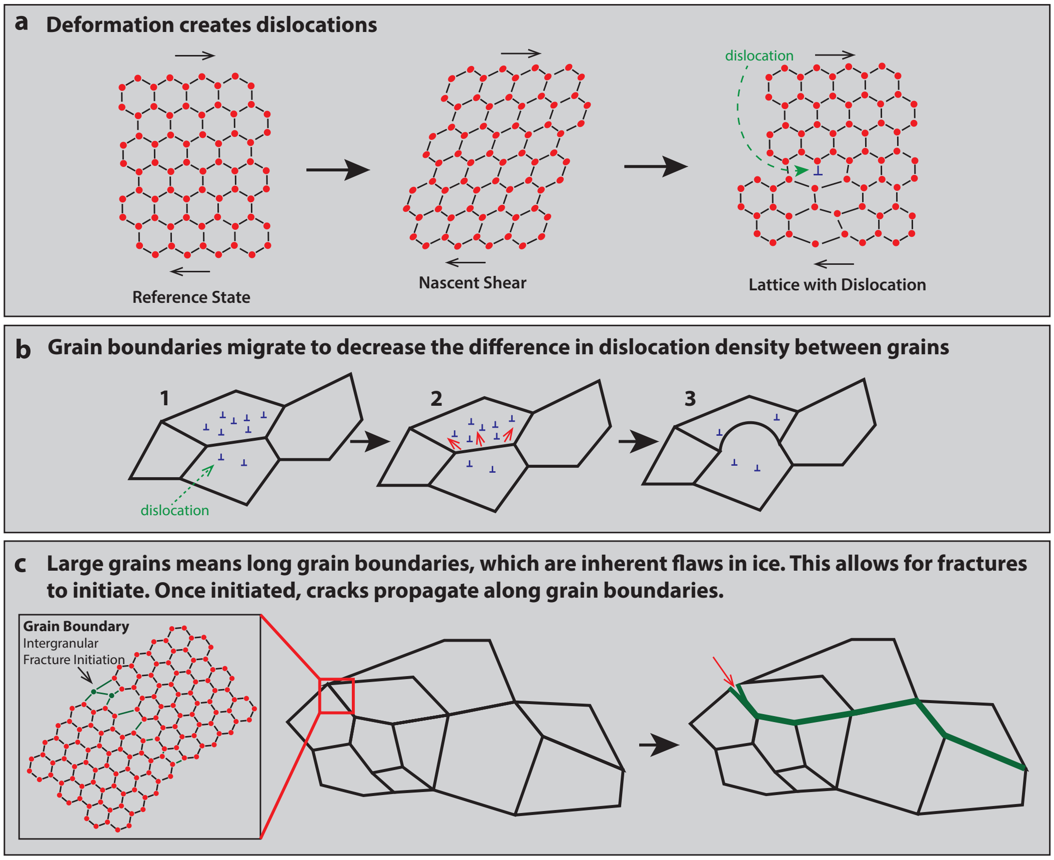

Figure 1: Schematic of migration recrystallization and its effect on ice strength. (a) In response to stress (in Antarctic glaciers, this stress arises from the ice sheet deforming under its own weight), the ice shears, creating dislocations. (b) A hypothetical polycrystalline ice of four grains. Due to local heterogeneities in stress, the density of the resulting dislocations are also heterogeneous [1]. To relieve stresses created by the difference in dislocation density between two grains, the grain boundary migrates towards the area of higher dislocation density [2], absorbing the dislocations and leaving behind a region of zero dislocation density [3]. The fact that the boundary leaves behind a region of no dislocation density may create more heterogeneities in dislocation density, driving further grain boundary migration. (c) Schematic that illustrates the role grain boundaries play in fracture. This shows a theoretical polycrystalline ice of 10 grains. Grain boundaries are inherent flaws in the ice because they interrupt the ordered structure of the lattice (inset). This enables initiation of intergranular fracture in response to stresses. Once the fracture is initiated, cracks propagate along grain boundaries because they are the weakest part of the ice. Outlined in green is a potential path a fracture may take.

Chapelle et al., 1998; De Bresser et al., 2001; Rios et al., 2005; Chauve et al., 2017). For many of these mechanisms, there are not explicit models or clear understanding of the physical processes. In this model, we parameterize the energy changes that occur during grain-size reduction and do not explicitly model specific mechanisms of grain-size reduction, as previous studies have done (Austin and Evans, 2007; Behn et al., 2020). Therefore, the estimates presented in this study may account for multiple physical processes of grain size reduction.

In the absence of deformation (static recrystallization), normal grain growth dominates, meaning that grain boundaries migrate outwards, leading to an increase in grain size (Alley, 1992). This migration is driven partially by grain boundary energy γ, which represents the change in free energy per change in unit area of the grain (Alley et al., 1986a,b). In contrast, deformation activates the two other recrystallization mechanisms (dynamic recrystallization) through the introduction of dislocations into the ice crystalline lattice. In an incompressible material such as ice, the rate of work done during deformation is defined as the double inner product $\tau_{ij}\dot{\epsilon}_{ij}$ (in summation notation), where τ_{ij} is the deviatoric stress tensor and $\dot{\epsilon}_{ij}$ is the strain rate tensor. The work rate is a combination of the change in internal energy from migration recrystallization and grain-size reduction, described mathematically as

$$(1-\Theta)\tau_{ij}\dot{\epsilon}_{ij} = \dot{E}_{\mathrm{red}} - \dot{E}_{\mathrm{mig}} \tag{2}$$

where Θ represents the fraction of the work rate that is dissipated as heat, $\dot{E}_{\mathrm{red}}$ is the rate of change in internal energy due to grain-size reduction, and $\dot{E}_{\mathrm{mig}}$ is the rate of change in internal energy due to migration recrystallization. While grain-size reduction reduces grain size, migration recrystallization grows grains: grain-scale stress gradients cause heterogeneity in dislocation density within the grain, which result in stress gradients that drive the outward migration of boundaries. This mechanism is dominant at high temperatures and high strain, where dislocation density is likely to be most heterogeneous (Duval, 1985; Alley, 1988). Since grain-size reduction and migration recrystallization have opposite effects on surface energy, the two energy rates have opposite signs (discussed more in detail in Supplement Section A).

Here, we build upon the steady-state grain size model from Austin and Evans (2007) by adding a parameterization for migration recrystallization, allowing us to predict grain size in shear margins. Migration recrystallization occurs when the temperature of the material approaches the melting temperature (Duval and Castelnau, 1995; Montagnat and Duval, 2000). Current steady-state grain size models, such as those derived by Derby and Ashby (1987), De Bresser et al. (1998), Hall and Parmentier (2003), and Austin and Evans (2007), were developed for solid earth studies and do not incorporate effects of migration recrystallization because rocks tend to deform at temperatures well below their melting temperatures. Ice on Earth is never more than a few tens of degrees colder than its melting temperature and thus deformation can warm ice to within a few degrees or less of its melting temperature (Meyer and Minchew, 2018), where we'd expect migration recrystallization to be most active.

2.1. Migration Recrystallization

The driving forces for migration recrystallization are the stress gradients created by heterogeneities in dislocation density that drive the outward migration of grain boundaries (Figure 1) (Derby and Ashby, 1987). Once the strain energy of grains exceeds the surface energy of the grain boundaries of an individual grain, recrystallization begins in a wave from regions of high strain energy and large gradients in strain energy (Duval et al., 1983; Alley, 1992). The grain boundaries of an individual grain migrate outwards to reduce the lattice strain energy. Recrystallization ceases when the boundary energy of the grain exceeds the lattice strain energy of the grain (Duval and Castelnau, 1995).

In this study, we derive a steady-state model and thus we consider the bulk properties of a macroscopic parcel of ice, rather than any localized discontinuities, when determining when migration recrystallization occurs. Since strain must be accumulated to generate dislocations, previous studies have assumed that this criterion is fulfilled for strains larger than $1-10\%$ (Duval and Castelnau, 1995). Strains of this magnitude are likely in shear margins of fast-flowing glaciers and we can expect that once ice has deformed sufficiently to warm the ice to $-10°$C, the ice has achieved strains of $1-10\%$. Thus, here we let temperature be a proxy for strain and assume migration recrystallization occurs for temperatures that exceed approximately $-10°$C, as suggested by previous works (Duval, 1981; Duval and Castelnau, 1995).

The temperature dependence of recrystallization kinetics are represented by the activation energies. Previous studies have shown that at temperatures above $-10°$C, the kinetics of creep and grain growth change discontinuously due to the formation of pre-melt film and the proximity to the melting point (Jacka and Li Jun, 1994; Dash et al., 2006). Here, we set the temperature dependence of activation energies for creep and grain growth accordingly, such that temperature plays a significant role in determining which creep mechanism is dominant.

Ice sheet-scale shear stresses drive deformation in lateral shear margins, which consequently increases the density of dislocations within grains (Figure 1). We can represent the driving force of migration recrystallization as the difference of energy associated with a dislocation density ρ_d (defined as the number of dislocations per unit surface area) between neighboring grains, expressed as (Duval et al., 1983; Derby and Ashby, 1987; Derby, 1992)

$$\Delta E_{\mathrm{dis}} = \frac{1}{2}\mu b^2 \Delta\rho_d \tag{3}$$

where μ is the shear modulus and b is the magnitude of the Burger's vector. We express the change in dislocation density as $\Delta\rho_d \approx (\frac{D}{d})^q \rho_d$, where q is an exponent to be defined, and D is the characteristic length scale over which we consider the change in dislocation density. This expression is physically justified by the fact that the length scale over which we consider changes in dislocation density is approximately the grain size d (Duval et al., 1983; Alley, 1992). The scaling of grain size by the characteristic length scale D gives us a term physically comparable to strain. We relate dislocation density to the applied shear stress τ_s as $\rho_d \approx \frac{\tau_s^2}{\mu^2 b^2}$. This relationship can be understood theoretically by equating the internal stress from dislocation density ρ_d with the stress applied to the material (Alley, 1992) and has been derived and applied in metals and ceramics studies (Duval et al., 1983).

Applying these expressions for the change in dislocation density and for dislocation density to Equation 3, we can find the change in energy associated with dislocation density, which is the driving force for migration recrystallization (F_{mig}):

$$F_{\text{mig}} = \Delta E_{\text{dis}} \approx \frac{1}{2}\Big(\frac{D}{d}\Big)^{q}\frac{\tau_s^2}{\mu} \tag{4}$$

We can find an expression for the change of grain size by considering the growth rate for grain boundary migration, which is equal to the velocity of migration, $v = MF_{mig}$, where M is the mobility of the grain boundary (Duval et al., 1983; Derby and Ashby, 1987; Derby, 1992). The mobility of grain boundaries is expressed as $M = M_0 \exp\big[-\frac{Q_m}{RT}\big]$, where Q_m is the activation energy for grain boundary mobility, R is the ideal gas constant, T is temperature, and M_0 is the intrinsic mobility (Higashi, 1978), defined here as $M_0 = 0.023$ m^4 J^{-1} s^{-1} (Llorens et al., 2017). The rate of change in internal strain energy due to migration recrystallization, $\dot{E}_{mig}$ (Equation 5), is the time derivative of Equation 4, represented as

$$\dot{E}_{\text{mig}} = -\frac{1}{2}\frac{\tau_s^2}{\mu}q\frac{D^q}{d^{q+1}}\dot{d}_{\text{mig}} \tag{5}$$

$$\dot{d}_{\text{mig}} = MF_{mig} = \frac{1}{2}\frac{\tau_s^2}{\mu}\frac{D^q}{d^q}M \tag{6}$$

with the corresponding rate of change in grain size given by Equation 6.

2.2. Normal Grain Growth

The expression for the increase in grain size from normal grain growth is well-established and derived from the change in surface energy that occurs due to the migration of a grain boundary (Alley et al., 1986a):

$$d^p = d_0^p + kt \tag{7}$$

where p is the grain-growth exponent (to be constrained), d_0 is the initial grain size, and k is the grain growth rate factor. The grain growth factor is parameterized by $k = k_0 \exp\left[-\frac{Q_{gg}}{RT}\right]$, where k_0 is an empirical prefactor and Q_{gg} is the activation energy for normal grain growth (Duval, 1985; Alley et al., 1986a; Jacka and Li Jun, 1994). The rate of change in grain size due to normal grain growth $\dot{d}_{nor}$ is the time-derivative of Equation 7.

2.3. Grain-size reduction

Grain-size reduction increases surface energy within a volume of a polycrystalline material (Duval and Castelnau, 1995). This change in surface energy is related to a geometric constant that represents the characteristic shape of grains, grain size, and grain boundary energy γ (Alley et al., 1986a; Austin and Evans, 2007). Grain boundary energy γ represents the change in free energy resultant from a change in area of the grain (Derby and Ashby, 1987), and laboratory experiments has found the value to be $\gamma = 0.065\ \frac{\mathrm{J}}{\mathrm{m}^2}$ (Ketcham and Hobbs, 1969). From this, the rate of change in internal energy density to grain-size reduction is given as the change in surface energy, as shown in Austin and Evans (2007):

$$\dot{E}_{\mathrm{red}} = \frac{-c\gamma}{d^2}\dot{d}_{\mathrm{red}} \tag{8}$$

2.4. Steady-State Grain Size

Grain size evolution is a function of current grain size for all three recrystallization mechanisms. In the case of normal grain growth and migration recrystallization, the exponents p and q respectively govern the rate of grain growth. We note that both normal grain growth and migration recrystallization occur by grain boundary migration. Since both recrystallization processes occur by the same process, with different driving forces, the change in grain size due to migration recrystallization and normal grain growth should have the same grain-size dependence. To represent this condition and to derive an expression for the steady-state grain size, we thus assume $q = \frac{p}{2}$. We then define the expression for steady-state grain size, accounting for the contribution of all mechanisms to grain size (Equation 1) and the mechanical work that goes into recrystallization (Equation 2):

$$d_{ss} = \left[\frac{\overbrace{4kp^{-1}c\gamma\mu^2}^{\text{Normal grain growth}} + \overbrace{\tau_s^4 D^p \left(\frac{p}{2}\right) M}^{\text{Migration recrystallization}}}{\underbrace{8(1-\Theta)\tau_s\dot{\epsilon}_s\mu^2}_{\text{Grain-Size Reduction}}} \right]^{\frac{1}{1+p}} \tag{9}$$

where $\dot{\epsilon}_s$ is the shear strain rate. The full derivation is found in Supplement Section A. The numerator consists of both grain growth mechanisms and the denominator describes the contribution of grain reduction, similar to relations derived previously (Derby and Ashby, 1987). Without any clear estimates for Θ, we assume $\Theta \approx 1$, implying that most of the work done during deformation drives changes in thermal energy that warm the ice, a common assumption made when studying shear margins of glaciers (Jacobson and Raymond, 1998; Suckale et al., 2014; Meyer and Minchew, 2018).

2.5. Model Validation

We use GRIP ice core temperature and grain size datasets (Gundestrup et al., 1993; Thorsteinsson et al., 1997; Johnsen et al., 1997) to benchmark our model due to the availability of grain size and temperature data. In benchmarking our model against ice cores, we focus on the lower ~ 500 m of the ice column where we expect vertical shearing to be the dominant component of deformation, as these are conditions that most closely match those of shear margins and it is the region in which migration recrystallization is expected to be most active. Since the parameterizations for normal grain growth and grain-size reduction are well-established (Alley et al., 1986a,b; Austin and Evans, 2007; Behn et al., 2020), the term for migration recrystallization is the main piece of the model that requires benchmarking. Therefore, possible inconsistencies between our model setup and the conditions at shallow depths (< 500 m) in GRIP do not adversely affect the comparison of our model to the data.

The depth profile of shear strain rate and shear stress come from a nonzero surface slope α, which drives ice deformation. The region of GRIP is approximately $3-4$ km away from an ice divide, whose position we estimated using a digital elevation model (ArcticDEM; (Porter et al., 2018)) and validated by previous work that used GPS data (Hvidberg et al., 1997). Close to ice divides (less than an ice thickness away from the ice divide; in the case of GRIP, 3 km), the strain rate is dominated by (normal) longitudinal strain, whereas further away from ice divides (more than an ice thickness from the divide), the strain rate becomes dominated by the vertical shear strain rate due to the ice being frozen to the bed (Raymond, 1983; Gundestrup et al., 1993; Hvidberg et al., 1997). Therefore, we take the vertical shear strain rate to be the dominant component of the strain rate tensor in the lower portion of the ice column and compute it from temperature and shear stress (Figure 2b). We compute vertical shear stress (taken to be equal to the gravitational driving stress) for $\alpha = 0.01^\circ$ and $\alpha = 0.05^\circ$, reasonable bounds on the surface slope in the region of the GRIP ice core (Helm et al., 2014). The grey shading represents the depth at which the ice has not yet reached steady state (dark grey for $\alpha = 0.05^\circ$, light grey for $\alpha = 0.01^\circ$), and therefore the models should not predict the correct grain sizes (Figure 2c). The independence of grain size model to conditions (temperature, shear strain rate, stress, grain size) at all other depths (Equation 9) prevents errors at shallower depths that may be attributable to unmodeled longitudinal strain rates or lack of steady state from propagating to deeper depths, which are being used to benchmark the model.

Our model is largely consistent with the grain size data from the GRIP ice core (Figure 2c). Near the bed, migration recrystallization is the dominant mechanism and thus responsible for the rapid increase in grain size. When applying our model, which incorporates the contributions of migration recrystallization, we see a reasonable fit to the GRIP ice core data near the bed. The depth at which grains begin to grow is largely dictated by temperature. At temperatures of approximately $-10^\circ C$, grain boundaries become more mobile, enabling high-velocity grain boundary migration (Duval and Castelnau, 1995; Urai et al., 1995). This critical temperature T_c at which this change in activation energy occurs has been experimentally determined. However, studies have shown that critical temperatures between $-8^\circ C$ and

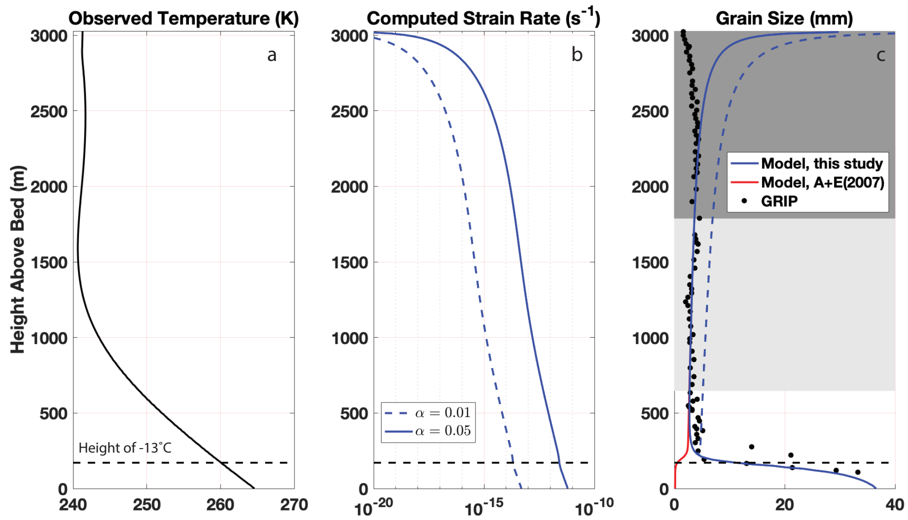

Figure 2: Results of a steady-state grain size model: (a) Temperature measured from the GRIP ice core, (b) strain rate computed from shear stress using the constitutive relation (Glen's Flow Law) for ice (where the flow-rate parameter is found from temperature by the Arrhenius relation and the flow-law exponent is taken to be $n = 3$ (Jezek et al., 1985) for surface slopes of 0.05° (solid line) and 0.01° (dashed line), (c) grain size computed from the model presented in this study from surface slopes of 0.05° (solid blue line) and 0.01° (dashed blue line), reasonable surface slopes for this region (Helm et al., 2014), the model presented in Austin and Evans (2007) (red line), and measured from the GRIP ice core (black circles). The grey shading represents the depths at which the ice has not yet reached steady-state (dark grey for a surface slope of 0.05° and light grey for a surface slope of 0.01°) and may be contaminated by firn processes. For shear margins, the most relevant areas are those that are in steady state and thus outside the grey shaded boxes (discussed further in Supplement Section D).

$-15°C$ may apply to natural conditions (Barnes et al., 1971; Goldsby and Kohlstedt, 2001; Kuiper et al., 2020). We show model estimates of grain size for a critical temperature of $T_c = -13°C$ (Figure 2), to demonstrate that defining a critical temperature within reasonable bounds of the canonical value of $-10°C$ produces an accurate estimate of the grain size profile. However, for the remainder of this study, we use the canonical value $T_c = -10°C$ for consistency with much of the salient literature referenced here. We show in Supplement Section B that the model provides a good fit to both GISP2 ice core data and WAIS Divide ice core data as well, showing that the model is applicable to different ice sheets and different regions.

The magnitude of the change in grain size with depth is controlled primarily by two parameters: the characteristic length-scale D and the grain growth exponent p (Equation 7). These two parameters are poorly constrained in natural deforming glacier ice. Traditionally, the grain growth exponent is taken to be $p = 2$ in glacier ice, from a fit to laboratory data and borehole measurements (Duval, 1985; Alley et al., 1986a,b). Recent work has shown that this value of the grain growth exponent best fits bubble-free glacier ice and that bubbled ice more likely has a higher grain growth exponent (Azuma et al., 2012). Since GRIP ice core is in a slowly-deforming region that is likely to have a higher concentration of bubbles, we use $p = 9$ for that fit. On the other hand, we are interested in rapidly-deforming regions that likely have a low concentration of bubbles, so we use $p = 2$ for the remainder of this study. We reserve for future work a complete exploration of the effect of varying grain growth exponents. The characteristic grain size D is uncertain as well, given that this is a scaling factor and the average grain size can vary widely in different parts of Antarctica. In the Supplement Section C, we show that values of D between 50 mm and 100 mm best represent the ice core data we use here, and we take $D = 50$ mm to approximate the best fit.

3. Model Results in Shear Margins

We first apply this model to a single column of an idealized shear margin in which the strain rate is constant with depth. We compute grain size from three different strain rates, representing a reasonable range of strain rates seen in shear margins of Antarctic ice streams (Alley et al., 2018). We compute ice temperature from strain rate using the thermomechanical model developed by Meyer and Minchew (2018) (Figure 3b) (with vertical accumulation accounted for in the Peclet number, where Pe = 2).

For a low strain rate ($\dot{\epsilon} = 6 \times 10^{-10}$ s^{-1}), temperature increases only slightly with depth and thus grain size remains relatively constant with depth. For an intermediate strain rate ($\dot{\epsilon} = 1.3 \times 10^{-9}$ s^{-1}), comparable to that found in shear margins of most ice streams in Antarctica, temperature increases significantly with depth, reaching the melting temperature approximately 100 m from the bed. Grains grow with depth until the critical temperature of $-10°C$, where there is a decrease in grain sizes due to an increase in the prevalence of grain-size reduction. There is then a rapid growth of grains due to temperatures approaching $-10°C$, when enough strain energy has built for grain boundaries to migrate through migration recrystallization. Below approximately 500 meters above the bed, grain sizes become roughly constant with depth due to strain rate and temperature increasing enough such that creep and subsequent grain reduction becomes more active and balances the contribution of migration recrystallization. For a high strain rate ($\dot{\epsilon} = 6 \times 10^{-8}$ s^{-1}), temperatures increase dramatically, reaching the melting point approximately 700 m above the bed. The ice remains temperate for the remainder of the ice column. Due to the dramatic increase in temperature in the first few hundred meters, grain size increases from $\sim$ 2 mm at the surface to $\sim$ 13 mm approximately 200 m from the surface. Grain sizes then remain roughly constant with depth for the remainder of the ice column. The estimate that grains are large in shear margins and regions where the ice is warm is supported by observations from Antarctic ice streams (Jackson and Kamb, 1997) and from temperate glaciers (Tison and Hubbard, 2000).

In contrast to our results, studies in the solid earth community have considered the effect of recrystallization on grain sizes in shear zones and found that grain size reduces in shear zones due to the dominance of grain-size reduction in regions with high strain rate (e.g. De Bresser et al. (2001); Montési and Hirth (2003)). Rocks in deformational zones are often far below their melting temperature, so a temperature increase by shear heating would have to be much larger than that for ice, which is everywhere close to its melting temperature. Ice temperatures near the melting point drive migration recrystallization on Earth, which results in a growth in grains in shear margins rather than a reduction in grain size.

3.1. Effect of Grain Size on Ice Rheology

Grain size affects the rheology of ice. Typically, ice rheology is described through a power-law relationship (Glen's flow law), which relates strain rate to stress raised to a power n, $\dot{\epsilon} = A\tau^n$. The value of n reflects the creep mechanism that ice deforms by and thus the choice of n in ice-flow modeling significantly affects the behavior of deforming ice. Uncertainties in the parameters of this flow law contribute significantly to uncertainties in large-scale ice-flow modeling, and constraining values of n is critical to making projections of ice sheet behavior.

Values of $n = 3$ are commonly used because this value fits laboratory data for the creep of ice (Jezek et al., 1985). However, a value of $n = 3$ does not clearly match with one creep mechanism. Instead, a flow law exponent of $n \approx 3$ may describe creep by a combination of dislocation creep ($n \approx 4$), which is grain-size-independent, and grain-boundary sliding ($n \approx 2$), which is grain-size-dependent (Montagnat and Duval, 2000; Goldsby and Kohlstedt, 2001; Behn et al., 2020). Deformation of ice with large grain sizes generally favors dislocation creep as the dominant deformation mechanism.

Dislocation creep occurs through dislocations, line defects in the ice, which enable planes of the ice crystalline lattice to move past each other. Migration recrystallization annihilates dislocations through the migration of grain boundaries, further increasing grain size and producing space for new dislocations to move through, which allows for continued dislocation creep. The rate of creep for grain-size-dependent deformation mechanisms (all except dislocation creep) is inversely related to grain size, so in ice with large grains, the rate of grain-size-dependent creep is likely to be low. Thus, as grains grow, the flow law tends to a power-law relationship with $n = 4$, describing dislocation creep as the sole creep mechanism.

This suggests that in areas of rapid deformation, such as the margins of ice streams, modeling ice flow with a flow-law exponent of $n \approx 4$ (dislocation-creep-dominant flow) may more accurately capture the dynamics occurring as the ice deforms, a result also estimated using satellite observations of ice shelves (Millstein and Minchew, 2020). In Supplement Section C, we show these results from our model for varying values of n. The value of n directly affects the rate of flow of ice, as viscosity scales with strain rate to the power of $\frac{1-n}{n}$. Thus, a value of $n = 4$ implies a lower viscosity for a given strain rate, suggesting that models may be overestimating the viscosity of ice in areas of rapid deformation.

3.2. Effect of grain size on fracture vulnerability

In the absence of pre-existing macro-scale fractures, the size of grains has a significant effect upon the strength of ice because grain boundaries are themselves flaws in the ice along which cracks can propagate (Schulson and Hibler, 1991). Intuitively, an increase in grain size translates to an increase in the length of grain boundaries, resulting in an increase in vulnerability to fracture (Figure 3a). Laboratory studies have similarly found that the tensile strength of ice σ_t, defined as the total stress required to fracture ice in tension, decreases with increasing grain size according to the following relationship: (Currier and Schulson, 1982; Schulson et al., 1984; Nixon and Schulson, 1988)

$$\sigma_t = Kd^{-\frac{1}{2}} \tag{10}$$

where K is a constant. While this is an empirical relationship, studies have developed theoretical bases for this relationship. The most prevalent explanation is the dislocation pileup mechanism, which explains deformation through the pileup of dislocations at the edge of a grain that then induces

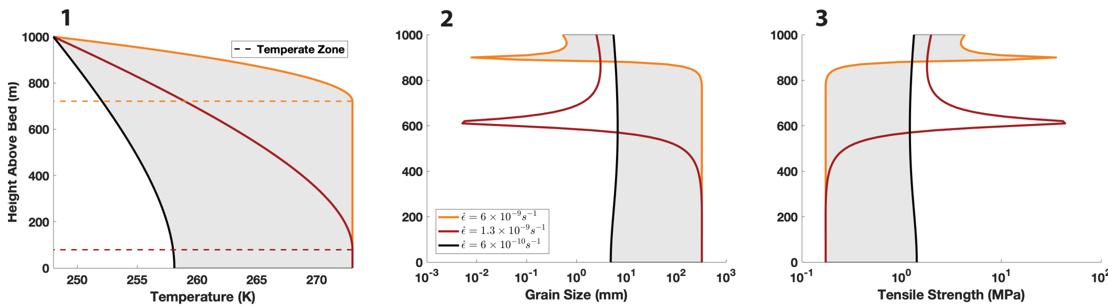

Figure 3: Results from an idealized model showing the relationship between ice temperature, grain size, and tensile strength. (1) Ice temperature computed from the thermomechanical model presented in Meyer and Minchew (2018), (2) Grain size computed from the steady-state grain size model developed here (Equation 9), (3) Tensile strength computed from Equation 10, for 3 strain rates.

deformation in a neighboring grain (Li and Chou, 1970). Fractures initiate to reduce the stress that forms due to this dislocation pileup. The stress required for this to occur has the same grain size dependence as that in Equation 10 (Li and Chou, 1970; Schulson et al., 1984).

We apply Equation 10 to compute the tensile strength of ice as a function of grain size (setting $K = 52$ kPa m$^{\frac{1}{2}}$ (Lee and Schulson, 1988)) for the case of the idealized shear margin (Figure 3b). For a low strain rate, since grain sizes remain approximately constant with depth, tensile strength also remains roughly constant with depth and $\sigma_t \approx 1.2$ MPa. For an intermediate strain rate, grain sizes grow between approximately 400 and 600 m above the bed before reaching a steady-state grain size of approximately 15 mm and then remaining constant with depth for the remainder of the ice column. Similarly, tensile strength remains constant until approximately 600 m above the bed. At this depth, tensile strength increases sharply due to a decrease in grain size, and then tensile strength decreases to approximately 0.4 MPa and remains constant with depth to the bed. At a high strain rate, tensile strength follows a similar pattern as that for intermediate strain rates, though the decrease in tensile strength occurs closer to the surface ($\sim$ 900 m height).

In locations of ice sheets in which the ice is frozen to the bed, a similar decrease in tensile strength will be likely near the bed due to an increase in grain size caused by migration recrystallization, as seen in the GRIP ice core (Figure 2). However, that decrease in tensile strength would be coupled with an increase in the overburden pressure, preventing tensile fractures from forming. In the case of shear margins, however, we observe a decrease in tensile strength to approximately 25% of the tensile strength a few hundreds of meters below the surface. With relatively low overburden pressure at these depths, this leaves a significant depth of the shear margin vulnerable to the propagation of microcracks along grain boundaries and thus the nucleation of large-scale fractures. Though not explicitly represented in these models, we would expect the water pressure at the base of ice shelves to facilitate the opening of tensile fractures, which renders the deeper portions of the shear margins on ice shelves, where tensile strength is lowest, quite vulnerable to fracture.

4. Application to Pine Island Glacier, West Antarctica

We apply our model to Pine Island Glacier in West Antarctica because of its rapid deformation and potential for large-scale implications for the Antarctic Ice Sheet (Wingham et al., 2009). The yearly velocity of Pine Island Glacier is found from LANDSAT 8 satellite imagery (Figure 4b) (Gardner et al., 2018), ice thickness is calculated from basal topography from BedMachine (Morlighem et al., 2020), and surface elevation from the Reference Elevation Model of Antarctica (Howat et al., 2019). We use surface mass balance, averaged over the years 1979-2019, from the RACMO model of Antarctica to set the rate of vertical advection in the thermomechanical model (Van Wessem et al., 2014). Results for other outlet glaciers in Antarctica are shown in Supplement Section F.

We compute grain size from surface strain rates (calculated from surface velocity; Figure 4b), ice temperature (calculated from surface strain rates), and ice thickness. Grain size is also dependent upon Θ, the fraction of work dissipated as heat. Commonly, it is assumed that all the work done during deformation is dissipated as heat, $\Theta \approx 1$ (Jacobson and Raymond, 1998; Suckale et al., 2014; Meyer and Minchew, 2018). However, the value has not been experimentally or theoretically constrained. Here, we present results for $\Theta \approx 1$ and in the Supplement Section F we present results with $\Theta = 0.5$ and $\Theta = 0.25$. The tensile strength of ice is then computed from grain size. We show three slices of the ice column: the grain size and tensile strength at 25% of the ice thickness, at 50% of the ice thickness, and 75% of the ice thickness (Figure 4c).

Grains are large in the shear margins of Pine Island Glacier ($\sim$ 12 mm) relative to the rest of the glacier and ice core data. This is likely due to high strain rates resulting in elevated ice temperatures (at or near the melting point). Previous studies show extensive zones of temperate ice in the shear margins of Pine Island Glacier (Meyer and Minchew, 2018), and this drives migration recrystallization and increases the size of grains. The depth profile

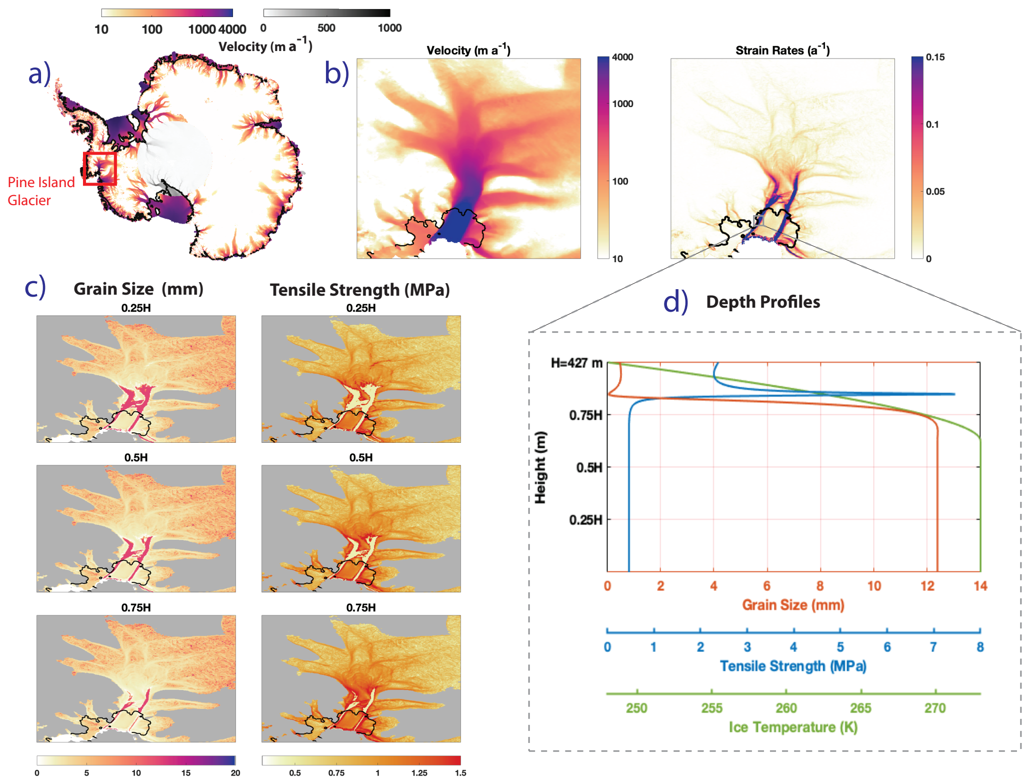

Figure 4: (a) Surface velocity of Antarctica from Landsat 7 and 8 (yellow to purple scale bar) (Gardner et al., 2018), with the pole hole filled in from NASA MEaSUREs (grey scale bar) (Mouginot et al., 2012; Rignot et al., 2017), with the region of Pine Island Glacier outlined in red. (b) Surface velocity and surface strain-rates of Pine Island Glacier. (c) Estimated grain sizes and tensile strength at varying depths: 25% of ice thickness (H) from the bed, 50% of ice thickness from the bed, and 75% of ice thickness from the bed. Areas where the model is not valid (flow speed < 30 m a^{-1}) are shown in grey. Here we show results for $\Theta \approx 1$, the assumption used in thermomechanical models of ice (Jacobson and Raymond, 1998; Suckale et al., 2014; Meyer and Minchew, 2018). Results using other values of Θ are shown in Supplement Section F. (d) Depth profilies of grain size, tensile strength, and ice temperature for a single point of the shear margin of the Pine Island Glacier ice shelf.

largely mirrors that seen in the idealized case (Figure 3b): at the bed, most of the margin contains coarse-grained ice. A similar area of coarse-grained ice exists at 25% of the ice thickness. In the middle of the ice column (50%), the area of coarse-grained ice thins but still spans a significant portion of the margin, especially upstream. Finally, near the surface (75% of ice thickness), the area of large grains thins even more but still dominates the shear margin (Figure 4c,d). In general, as seen in Figure 4d, grain sizes remain constant with depth beyond the region near the surface and therefore the profiles in Figure 4c show the region of grain growth expanding as temperatures increase with depth. The difference between grain size in the margins and grain size in the trunk of the ice stream decreases as Θ decreases (as less work is dissipated as heat). Even at low Θ, grains are still larger in the margins (Supplement Section F). This may imply that, in the margins, dislocation creep is the dominant deformation mechanism and thus modeling the evolution of Pine Island Glacier using $n = 4$ in the margins is most accurate.

Large grain sizes in the margins translate to relatively low values of tensile strength. Tensile strength drops from ~ 1.5 MPa in the fine-grained regions to ~ 0.2 MPa in the coarse-grained regions. These values are significantly lower than some estimated tensile strength values for relatively pristine and undeformed ice (Ultee et al., 2020) and within the range of reasonable values found by other studies (Vaughan, 1993). Furthermore, there is a significant portion of the shear margin that has very low tensile strength near the surface (75% of ice thickness). A reduction in tensile strength occurs for low values of Θ as well, though the reduction is not as significant and does not extend as far up the ice column (Supplement Section F). This dramatic drop in tensile strength, particularly near the surface, may increase the vulnerability of the shear margin to fracture and is positioned approximately where significant damage and fracturing in Pine Island Glacier have been observed (Lhermitte et al., 2020). Ice shelves are particularly vulnerable to changes in tensile strength because basal crevasses are more easily formed than in grounded ice due to the fact that the cracks are water-filled. A reduction in the strength of ice at the base of the ice column may increase the vulnerability of ice shelves significantly relative to grounded ice since it allows for cracks to propagate from the base of the ice shelf and may allow for full-thickness fractures to develop. This drop in tensile strength is due to the rate of deformation in shear margins, and so as Pine Island Glacier accelerates in a changing climate, the ice shelf of Pine Island Glacier may become more vulnerable to fracture and calving events (Wingham et al., 2009).

5. Conclusions

In this study, we show that grain sizes in shear margins are large relative to slower deforming regions, which influences the rate of creep and vulnerability to fracture of the ice and may contribute to accelerated flow and instability of ice shelves. To show this, we derive a new model for steady-state grain size that accounts for migration recrystallization, a mechanism for recrystallization that is dominant at high strain rate and high temperature and results in an increase in grain size. Our model demonstrates that migration recrystallization is dominant in shear margins and thus ice grains in shear margins are large ($\sim$ 12 mm), compared to grain sizes of $\sim 2-7$ mm in surrounding regions. This is a significant deviation from previous work in solid earth recrystallization studies that have shown shear zones of rock to be fine-grained. This distinction arises because ice in terrestrial glaciers and ice sheets is close to its melting temperature and thus migration recrystallization can outpace grain-size reduction, resulting in coarse grains in shear zones. We show here that this result has implications for the vulnerability of shear margins to fracture and the rheology of ice in shear margins.

The flow of ice is described by a constitutive relation that relates strain rate and stress through a power law, with a flow exponent n. The value of $n = 3$ has been found to match laboratory data and is commonly used in ice sheet and ice flow models. However, we suggest here that in shear margins where grain sizes are large, dislocation creep ($n = 4$) is likely to be the dominant deformation mechanism, since large grain sizes give more area for slip to occur through dislocations and large grain sizes also reduce the rates of creep by mechanisms such as grain-boundary sliding and diffusion creep. Thus, a flow law exponent of $n \approx 4$ may be more appropriate than the commonly-used $n = 3$ for rapidly-deforming regions of ice streams, such as the lateral margins. This may imply that, by using the traditional Glen's flow law with $n = 3$ in large-scale ice flow models, we are underestimating the rate of creep, and consequently the acceleration of flow, in key regions of Antarctica. While we do not directly model the effects of dynamic recrystallization on fabric development here, including fabric is likely to strengthen this result due to the creation of a single-maximum fabric that softens the ice and allows for higher rates of deformation. Further, it is well known that an increase in grain size reduces the strength of polycrystalline materials. Here, we show that the tensile strength of ice in shear margins of Pine Island Glacier, West Antarctica are approximately 25% of the tensile strength of ice in the centerline of the glacier. This decrease in tensile strength may give rise to damage and fracture that previous studies have identified in Pine Island Glacier (Lhermitte et al., 2020). Further, this model produces predictions of grain size that can be tested by observations of grain size in shear margins.

This new understanding of recrystallization in shear zones may provide a way to estimate more accurately the vulnerability of rapidly deforming glaciers to instability by parameterizing the effect of dynamic recrystallization processes in large-scale ice flow models. This work provides inroads into thinking about how to represent different types of flow in large-scale ice flow models with a spatially varying flow exponent n. Finally, this work suggests that dynamic recrystallization processes significantly affect the physical properties and dynamics of rapidly-deforming glaciers, and further work will consider the role that dynamic recrystallization and grain-scale processes play in the large-scale dynamics and energetics of shear margins.

Acknowledgements

We acknowledge enlightening conversations and feedback from Maurine Montagnat, Brian Evans, and Mark Behn, along with feedback from the MIT Glaciers Group. M.I.R. gratefully acknowledges funding from the Martin Fellowship and the Sven Treitel Fellowship. B.M. acknowledges funding from two NSF-NERC grants, award numbers 1739031 and 1853918, and a grant from the NEC Corporation Fund for Research in Computers and Computation. No new data were produced for this study, and data used in this study are publicly available through their respective publications, cited here. The

code for the model and that generates the figures in this paper can be found at: https://github.com/megr090/grain-size-tensile-strength-model.

References

Alley, K.E., Scambos, T.A., Anderson, R.S., Rajaram, H., Pope, A., Haran, T.M., 2018. Continent-wide estimates of Antarctic strain rates from Landsat 8-derived velocity grids. Journal of Glaciology 64, 321–332. doi:10.1017/jog.2018.23.

Alley, R., 1988. Fabrics in Polar Ice Sheets: Development and Prediction. Science 240, 493–495. URL: https://www.sciencemag.org/lookup/doi/10.1126/science.240.4851.493, doi:10.1126/science.240.4851.493.

Alley, R., 1992. Flow-law hypotheses for ice-sheet modeling. Journal of Glaciology 38, 245–256. URL: https://www.cambridge.org/core/product/identifier/S0022143000003658/type/journal{_}article, doi:10.3189/S0022143000003658.

Alley, R., Perepezko, J., Bentley, C., 1986a. Grain Growth in Polar Ice: I. Theory. Journal of Glaciology 32, 425–433. doi:10.3189/s0022143000012132.

Alley, R., Perepezko, J., Bentley, C., 1986b. Grain Growth in Polar Ice: II. Application. Journal of Glaciology 32, 425–433. URL: https://www.cambridge.org/core/product/identifier/S0022143000012132/type/journal{_}article, doi:10.3189/S0022143000012132.

Austin, N.J., Evans, B., 2007. Paleowattmeters: A scaling relation for dynamically recrystallized grain size. Geology 35, 343. URL: https://pubs.geoscienceworld.org/geology/article/35/4/343-346/129818, doi:10.1130/G23244A.1.

Azuma, N., Miyakoshi, T., Yokoyama, S., Takata, M., 2012. Impeding effect of air bubbles on normal grain growth of ice. Journal of Structural Geology 42, 184–193. URL: http://dx.doi.org/10.1016/j.jsg.2012.05.005https://linkinghub.elsevier.com/retrieve/pii/S019181411200123X, doi:10.1016/j.jsg.2012.05.005.

Barnes, P., Tabor, D., Walker, J.C.F., 1971. The friction and creep of polycrystalline ice. Proceedings of the Royal Society of London. A. Mathematical and Physical Sciences 324, 127–155. URL: https://royalsocietypublishing.org/doi/10.1098/rspa.1971.0132, doi:10.1098/rspa.1971.0132.

Behn, M.D., Goldsby, D.L., Hirth, G., 2020. The role of grain-size evolution on the rheology of ice: Implications for reconciling laboratory creep data and the Glen flow law. The Cryosphere Discussions , 1–31URL: https://tc.copernicus.org/preprints/tc-2020-295/, doi:10.5194/tc-2020-295.

Chauve, T., Montagnat, M., Barou, F., Hidas, K., Tommasi, A., Mainprice, D., 2017. Investigation of nucleation processes during dynamic recrystallization of ice using cryo-EBSD. Philosophical Transactions of the Royal Society A: Mathematical, Physical and Engineering Sciences 375. doi:10.1098/rsta.2015.0345.

Cuffey, K.M., Thorsteinsson, T., Waddington, E.D., 2000. A renewed argument for crystal size control of ice sheet strain rates. Journal of Geophysical Research: Solid Earth 105, 27889–27894. URL: http://doi.wiley.com/10.1029/2000JB900270, doi:10.1029/2000JB900270.

Currier, J., Schulson, E., 1982. The tensile strength of ice as a function of grain size. Acta Metallurgica 30, 1511–1514. URL: https://linkinghub.elsevier.com/retrieve/pii/0001616082901717, doi:10.1016/0001-6160(82)90171-7.

Dash, J.G., Rempel, A.W., Wettlaufer, J.S., 2006. The physics of premelted ice and its geophysical consequences. Reviews of Modern Physics 78, 695–741. doi:10.1103/RevModPhys.78.695.

De Bresser, J., Ter Heege, J., Spiers, C., 2001. Grain size reduction by dynamic recrystallization: can it result in major rheological weakening? International Journal of Earth Sciences 90, 28–45. URL: http://link.springer.com/10.1007/s005310000149, doi:10.1007/s005310000149.

De Bresser, J.H.P., Peach, C.J., Reijs, J.P.J., Spiers, C.J., 1998. On dynamic recrystallization during solid state flow: Effects of stress and temperature. Geophysical Research Letters 25, 3457–3460. URL: http://doi.wiley.com/10.1029/98GL02690, doi:10.1029/98GL02690.

De La Chapelle, S., Castelnau, O., Lipenkov, V., Duval, P., 1998. Dynamic recrystallization and texture development in ice as revealed by the study of deep ice cores in Antarctica and Greenland. Journal of Geophysical

Research: Solid Earth 103, 5091–5105. URL: http://doi.wiley.com/10.1029/97JB02621, doi:10.1029/97JB02621.

Derby, B., 1992. Dynamic recrystallisation: The steady state grain size. Scripta Metallurgica et Materialia 27, 1581–1585. URL: https://linkinghub.elsevier.com/retrieve/pii/0956716X92901488, doi:10.1016/0956-716X(92)90148-8.

Derby, B., Ashby, M., 1987. On dynamic recrystallisation. Scripta Metallurgica 21, 879–884. URL: https://linkinghub.elsevier.com/retrieve/pii/0036974887903413, doi:10.1016/0036-9748(87)90341-3.

Duval, P., 1981. Creep and Fabrics of Polycrystalline Ice Under Shear and Compression. Journal of Glaciology 27, 129–140.

Duval, P., 1985. Grain growth and mechanical behaviour of polar ice. Annals of Glaciology , 3–6.

Duval, P., Ashby, M.F., Anderman, I., 1983. Rate-controlling processes in the creep of polycrystalline ice. Journal of Physical Chemistry 87, 4066–4074. doi:10.1021/j100244a014.

Duval, P., Castelnau, O., 1995. Dynamic recrystallization of ice in polar ice sheets. Journal de Physique IV 5, 197–205. URL: http://www.scopus.com/inward/record.url?eid=2-s2.0-33750590172{\&}partnerID=MN8TOARS, doi:10.1051/jp4.

Duval, P., Gac, H.L., 1980. Does the Permanent Creep-Rate of Polycrystalline Ice Increase with Crystal Size? Journal of Glaciology 25, 151–158. doi:10.3189/s0022143000010364.

Gardner, A.S., Moholdt, G., Scambos, T., Fahnstock, M., Ligtenberg, S., van den Broeke, M., Nilsson, J., 2018. Increased West Antarctic and unchanged East Antarctic ice discharge over the last 7 years. The Cryosphere 12, 521–547. URL: https://tc.copernicus.org/articles/12/521/2018/, doi:10.5194/tc-12-521-2018.

Goldsby, D.L., Kohlstedt, D.L., 2001. Superplastic deformation of ice: Experimental observations. Journal of Geophysical Research: Solid Earth 106, 11017–11030. URL: http://doi.wiley.com/10.1029/2000JB900336, doi:10.1029/2000JB900336.

Gow, A.J., Meese, D.A., Alley, R.B., Fitzpatrick, J.J., Anandakrishnan, S., Woods, G.A., Elder, B.C., 1997. Physical and structural properties of the Greenland Ice Sheet Project 2 ice core: A review. Journal of Geophysical Research: Oceans 102, 26559–26575. URL: http://doi.wiley.com/10.1029/97JC00165, doi:10.1029/97JC00165.

Gudmundsson, G.H., Paolo, F.S., Adusumilli, S., Fricker, H.A., 2019. Instantaneous Antarctic ice sheet mass loss driven by thinning ice shelves. Geophysical Research Letters 46, 13903–13909. URL: https://onlinelibrary.wiley.com/doi/abs/10.1029/2019GL085027, doi:10.1029/2019GL085027.

Gundestrup, N., Dahl-Jensen, D., Johnsen, S., Rossi, A., 1993. Borehole survey at dome GRIP 1991. Cold Regions Science and Technology 21, 399–402. URL: https://linkinghub.elsevier.com/retrieve/pii/0165232X9390015Z, doi:10.1016/0165-232X(93)90015-Z.

Hall, C.E., Parmentier, E.M., 2003. Influence of grain size evolution on convective instability. Geochemistry, Geophysics, Geosystems 4. URL: http://doi.wiley.com/10.1029/2002GC000308, doi:10.1029/2002GC000308.

Helm, V., Humbert, A., Miller, H., 2014. Elevation and elevation change of Greenland and Antarctica derived from CryoSat-2. The Cryosphere 8, 1539–1559. URL: https://tc.copernicus.org/articles/8/1539/2014/, doi:10.5194/tc-8-1539-2014.

Higashi, A., 1978. Structure and Behaviour of Grain Boundaries in Polycrystalline Ice. Journal of Glaciology 21, 589–605. URL: https://www.cambridge.org/core/product/identifier/S0022143000033712/type/journal{_}article, doi:10.3189/S0022143000033712.

Howat, I.M., Porter, C., Smith, B.E., Noh, M.J., Morin, P., 2019. The Reference Elevation Model of Antarctica. The Cryosphere 13, 665–674. URL: https://tc.copernicus.org/articles/13/665/2019/, doi:10.5194/tc-13-665-2019.

Hruby, K., Gerbi, C., Koons, P., Campbell, S., Martín, C., Hawley, R., 2020. The impact of temperature and crystal orientation fabric on the dynamics of mountain glaciers and ice streams. Journal of Glaciology 66, 755–765. URL: https://www.cambridge.org/core/product/identifier/S0022143020000441/type/journal{_}article, doi:10.1017/jog.2020.44.

Hvidberg, C.S., Dahl-Jensen, D., Waddington, E.D., 1997. Ice flow between the Greenland Ice Core Project and Greenland Ice Sheet Project 2 boreholes in central Greenland. Journal of Geophysical Research: Oceans 102, 26851–26859. doi:10.1029/97JC00268.

Jacka, T., 1984. Laboratory studies on relationships between ice crystal size and flow rate. Cold Regions Science and Technology 10, 31–42. URL: https://linkinghub.elsevier.com/retrieve/pii/0165232X84900314, doi:10.1016/0165-232X(84)90031-4.

Jacka, T.H., Li Jun, 1994. The steady-state crystal size of deforming ice. Annals of Glaciology 20, 13–18.

Jackson, M., Kamb, B., 1997. The marginal shear stress of Ice Stream B , West Antarctica. Journal of Glaciology 43, 415–426.

Jacobson, H.P., Raymond, C.F., 1998. Thermal effects on the location of ice stream margins. Journal of Geophysical Research: Solid Earth 103, 12111–12122. URL: http://doi.wiley.com/10.1029/98JB00574, doi:10.1029/98JB00574.

Jezek, K., Alley, R., Thomas, 1985. Rheology of Glacier Ice. Science 227, 1335–1337. URL: https://www.sciencemag.org/lookup/doi/10.1126/science.227.4692.1335, doi:10.1126/science.227.4692.1335.

Johnsen, S., Clausen, H.B., Dansgaard, W., Gundestrup, N.S., Hammer, C.U., Andersen, U., Andersen, K.K., Hvidberg, C.S., Steffensen, P., White, J., Jouzel, J., Fisher, D., 1997. The Delta 18O along the Greenland Ice Core Project deep ice core and the problem of possible Eemian climatic instability. Journal of Geophysical Research 102, 26,397 – 26,410.

Ketcham, W.M., Hobbs, P.V., 1969. An experimental determination of the surface energies of ice. Philosophical Magazine 19, 1161–1173. doi:10.1080/14786436908228641.

Kuiper, E.J.N., De Bresser, J.H., Drury, M.R., Eichler, J., Pennock, G.M., Weikusat, I., 2020. Using a composite flow law to model deformation in the NEEM deep ice core, Greenland-Part 2: The role of grain size and premelting on ice deformation at high homologous temperature. Cryosphere 14, 2449–2467. doi:10.5194/tc-14-2449-2020.

Lee, R.W., Schulson, E.M., 1988. The Strength and Ductility of Ice Under Tension. Journal of Offshore Mechanics and Arctic Engineering 110, 187–191. URL: https://asmedigitalcollection.asme.org/offshoremechanics/article/110/2/187/435450/The-Strength-and-Ductility-of-Ice-Under-Tension, doi:10.1115/1.3257049.

Lhermitte, S., Sun, S., Shuman, C., Wouters, B., Pattyn, F., Wuite, J., Berthier, E., Nagler, T., 2020. Damage accelerates ice shelf instability and mass loss in Amundsen Sea Embayment. Proceedings of the National Academy of Sciences 117, 24735–24741. URL: http://www.pnas.org/lookup/doi/10.1073/pnas.1912890117, doi:10.1073/pnas.1912890117.

Li, J.C.M., Chou, Y.T., 1970. The role of dislocations in the flow stress grain size relationships. Metallurgical and Materials Transactions B 1, 1145. URL: http://link.springer.com/10.1007/BF02900225, doi:10.1007/BF02900225.

Llorens, M.G., Griera, A., Steinbach, F., Bons, P.D., Gomez-Rivas, E., Jansen, D., Roessiger, J., Lebensohn, R.A., Weikusat, I., 2017. Dynamic recrystallization during deformation of polycrystalline ice: insights from numerical simulations. Philosophical Transactions of the Royal Society A: Mathematical, Physical and Engineering Sciences 375, 20150346. URL: https://royalsocietypublishing.org/doi/10.1098/rsta.2015.0346, doi:10.1098/rsta.2015.0346.

MacAyeal, D.R., 1989. Large-scale ice flow over a viscous basal sediment: Theory and application to ice stream B, Antarctica. Journal of Geophysical Research: Solid Earth 94, 4071–4087. URL: http://doi.wiley.com/10.1029/JB094iB04p04071, doi:10.1029/JB094iB04p04071.

Meyer, C.R., Minchew, B.M., 2018. Temperate ice in the shear margins of the Antarctic Ice Sheet: Controlling processes and preliminary locations. Earth and Planetary Science Letters 498, 17–26. URL: https://doi.org/10.1016/j.epsl.2018.06.028https://linkinghub.elsevier.com/retrieve/pii/S0012821X18303790, doi:10.1016/j.epsl.2018.06.028.

Millstein, J., Minchew, B., 2020. Inferring ice rheology in Antarctic ice shelves using remotely-sensed surface velocity and ice thickness observations. AGU Fall Meeting 2020 .

Montagnat, M., Duval, P., 2000. Rate controlling processes in the creep of polar ice, influence of grain boundary migration associated with recrystallization. Earth and Planetary Science Letters 183, 179–186. URL: https://

linkinghub.elsevier.com/retrieve/pii/S0012821X00002624, doi:10.1016/S0012-821X(00)00262-4.

Montési, L.G., Hirth, G., 2003. Grain size evolution and the rheology of ductile shear zones: from laboratory experiments to postseismic creep. Earth and Planetary Science Letters 211, 97–110. URL: https://linkinghub.elsevier.com/retrieve/pii/S0012821X03001961, doi:10.1016/S0012-821X(03)00196-1.

Morlighem, M., Rignot, E., Binder, T., Blankenship, D., Drews, R., Eagles, G., Eisen, O., Ferraccioli, F., Forsberg, R., Fretwell, P., Goel, V., Greenbaum, J.S., Gudmundsson, H., Guo, J., Helm, V., Hofstede, C., Howat, I., Humbert, A., Jokat, W., Karlsson, N.B., Lee, W.S., Matsuoka, K., Millan, R., Mouginot, J., Paden, J., Pattyn, F., Roberts, J., Rosier, S., Ruppel, A., Seroussi, H., Smith, E.C., Steinhage, D., Sun, B., den Broeke, M.R., Ommen, T.D., van Wessem, M., Young, D.A., 2020. Deep glacial troughs and stabilizing ridges unveiled beneath the margins of the Antarctic ice sheet. Nature Geoscience 13, 132–137. URL: http://dx.doi.org/10.1038/s41561-019-0510-8, doi:10.1038/s41561-019-0510-8.

Mouginot, J., Scheuch, B., Rignot, E., 2012. Mapping of ice motion in antarctica using synthetic-aperture radar data. Remote Sensing 4, 2753–2767. doi:10.3390/rs4092753.

Nixon, W., Schulson, E., 1987. A Micromechanical view of the fracture toughness of ice. Le Journal de Physique Colloques 48, C1–313–C1–319. URL: http://www.edpsciences.org/10.1051/jphyscol:1987144, doi:10.1051/jphyscol:1987144.

Nixon, W.A., Schulson, E.M., 1988. The Fracture Toughness of Ice Over a Range of Grain Sizes. Journal of Offshore Mechanics and Arctic Engineering 110, 192–196. URL: https://asmedigitalcollection.asme.org/offshoremechanics/article/110/2/192/435461/The-Fracture-Toughness-of-Ice-Over-a-Range-of, doi:10.1115/1.3257050.

Pollard, D., DeConto, R.M., Alley, R.B., 2015. Potential Antarctic Ice Sheet retreat driven by hydrofracturing and ice cliff failure. Earth and Planetary Science Letters 412, 112–121. URL: http://dx.doi.org/10.1016/j.epsl.2014.12.035https://linkinghub.elsevier.com/retrieve/pii/S0012821X14007961, doi:10.1016/j.epsl.2014.12.035.

Porter, C., Morin, P., Howat, I., Noh, M.J., Bates, B., Peterman, K., Keesey, S., Schlenk, M., Gardiner, J., Tomko, K., Willis, M., Kelleher, C., Cloutier, M., Husby, E., Foga, S., Nakamura, H., Platson, M., Wethington, M.J., Williamson, C., Bauer, G., Enos, J., Arnold, G., Kramer, W., Becker, P., Doshi, A., D'Souza, C., Cummens, P., Laurier, F., Bojesen, M., 2018. ArcticDEM. doi:10.7910/DVN/OHHUKH.

Ranganathan, M., Minchew, B., Meyer, C.R., Gudmundsson, G.H., 2021. A new approach to inferring basal drag and ice rheology in ice streams, with applications to West Antarctic Ice Streams. Journal of Glaciology 67, 229–242. URL: https://www.cambridge.org/core/product/identifier/S0022143020000957/type/journal{_}article, doi:10.1017/jog.2020.95.

Raymond, C.F., 1983. Deformation in the vicinity of ice divides. Journal of Glaciology 29, 357–373. doi:10.1017/S0022143000030288.

Rignot, E., Mouginot, J., Scheuchl, B., 2017. MEaSUREs InSAR-Based Antarctica Ice Velocity Map, Version 2. doi:https://doi.org/10.5067/D7GK8F5J8M8R.

Rios, P.R., Siciliano Jr, F., Sandim, H.R.Z., Plaut, R.L., Padilha, A.F., 2005. Nucleation and growth during recrystallization. Materials Research 8, 225–238. URL: http://www.scielo.br/scielo.php?script=sci{_}arttext{\&}pid=S1516-14392005000300002{\&}lng=en{\&}tlng=en, doi:10.1590/S1516-14392005000300002.

Schulson, E.M., Hibler, W.D., 1991. The fracture of ice on scales large and small: Arctic leads and wing cracks. Journal of Glaciology 37, 319–322. URL: https://www.cambridge.org/core/product/identifier/S0022143000005748/type/journal{_}article, doi:10.1017/S0022143000005748.

Schulson, E.M., Lim, P.N., Lee, R.W., 1984. A brittle to ductile transition in ice under tension. Philosophical Magazine A: Physics of Condensed Matter, Structure, Defects and Mechanical Properties 49, 353–363. doi:10.1080/01418618408233279.

Suckale, J., Platt, J.D., Perol, T., Rice, J.R., 2014. Deformation-induced melting in the margins of the West Antarctic ice streams. Journal of Geophysical Research: Earth Surface 119, 1004–1025. URL: http://doi.wiley.com/10.1002/2013JF003008, doi:10.1002/2013JF003008.

Thomas, R.H., Bentley, C.R., 1978. A model for Holocene retreat of the West Antarctic Ice Sheet. Quaternary Research 10, 150–170. doi:10.1016/0033-5894(78)90098-4.

Thorsteinsson, T., Kipfstuhl, J., Miller, H., 1997. Textures and fabrics in the GRIP ice core. Journal of Geophysical Research: Oceans 102, 26583–26599. doi:10.1029/97JC00161.

Tison, J.L., Hubbard, B., 2000. Ice crystallographic evolution at a temperate glacier: Glacier de Tsanfleuron, Switzerland. Geological Society Special Publication 176, 23–38. doi:10.1144/GSL.SP.2000.176.01.03.

Ultee, L., Meyer, C., Minchew, B., 2020. Tensile strength of glacial ice deduced from observations of the 2015 eastern Skaftá cauldron collapse, Vatnajökull ice cap, Iceland. Journal of Glaciology 66, 1024–1033. URL: https://www.cambridge.org/core/product/identifier/S0022143020000659/type/journal{_}article, doi:10.1017/jog.2020.65.

Urai, J., Means, W., Lister, G., 1995. Dynamic Recrystallization of Minerals. Geophysical Monograph Series 36, 332–347.

Van der Wal, D., Chopra, P., Drury, M., Gerald, J.F., 1993. Relationships between dynamically recrystallized grain size and deformation conditions in experimentally deformed olivine rocks. Geophysical Research Letters 20, 1479–1482. doi:10.1029/93GL01382.

Van Wessem, J.M., Reijmer, C.H., Morlighem, M., Mouginot, J., Rignot, E., Medley, B., Joughin, I., Wouters, B., Depoorter, M.A., Bamber, J.L., Lenaerts, J.T., Van De Berg, W.J., Van Den Broeke, M.R., Van Meijgaard, E., 2014. Improved representation of East Antarctic surface mass balance in a regional atmospheric climate model. Journal of Glaciology 60, 761–770. doi:10.3189/2014JoG14J051.

Vaughan, D.G., 1993. Relating the occurrence of crevasses to surface strain rates. Journal of Glaciology 39, 255–266. URL: https://www.cambridge.org/core/product/identifier/S0022143000015926/type/journal{_}article, doi:10.1017/S0022143000015926.

Wingham, D.J., Wallis, D.W., Shepherd, A., 2009. Spatial and temporal evolution of Pine Island Glacier thinning, 1995-2006. Geophysical Research Letters 36, 5–9. doi:10.1029/2009GL039126.